

# Associations Between Spherical Particles of Two Dissimilar Phases

D. T. GAWNE\*

*Research Centre, British Steel Corporation, Port Talbot, Glamorgan, UK*

G. T. HIGGINS\*

*Illinois Institute of Technology, Chicago, Ill. 60616, USA*

An analysis is presented to assess the relationships between particles distributed throughout a medium. The adopted approach is to compare the observed data with the expected associations between particles calculated on the basis of random positioning. Since bulk structures are often examined by using a sectioning technique, the paper includes a method to transform two-dimensional observations into three-dimensional associations. This is achieved by assuming that the most complex association observed is the most complex association in the bulk material; the contributions to lower-order associations from this association are calculated and subtracted from the observed frequencies. The process is repeated, making the same assumptions about the next most complex association, and so on until a corrected matrix of associations has been compiled.

The analysis is applied to a partially recrystallised iron-0.4 wt % carbon alloy to give a complete description of the associations between carbide particles and recrystallised grains. In particular, it is shown that carbide particles are exclusive nucleation sites for recrystallisation.

## 1. Introduction

Associations between particles and the inference of three-dimensional arrangements from two-dimensional observations is a topic applicable to a number of scientific disciplines. The analysis presented in this paper was prompted by the needs of an experimental investigation into recrystallisation in steel.

Recrystallisation is the nucleation of new grains within a deformed material and their subsequent growth to consume the whole of the original defective structure [1]. It has been established experimentally [2] that recrystallisation is more rapid in iron containing a dispersion of spheroidal carbide ( $\text{Fe}_3\text{C}$ ) particles than in the pure metal. In order to understand the physical basis of this behaviour an electron microscopic study was initiated to establish the cause of the acceleration. As a part of this study it was considered necessary to determine the degree to which nuclei were associated with

carbide particles during the early stages of recrystallisation.

In this, as in many cases, the bulk material cannot be examined directly and a sectioning technique must be employed. The examination may be accomplished on polished planar sections using optical microscopy or on thin sections using electron microscopy. The latter course was chosen for the current investigation.

Observations upon thin sections of the partially recrystallised alloy indicate that some carbide particles are associated with recrystallised grains as shown in figs. 1 and 2, whilst others are not. However, even in the absence of any effect of particles upon recrystallisation, some recrystallised grains would still appear adjacent to carbide particles purely by random positioning. Conversely, if every particle in the bulk material were in contact with recrystallised grains in a section, a substantial proportion of particles would appear dissociated from recrystallised

\*Formerly of the Department of Metallurgy and Materials Science, University of Liverpool, England where the work was carried out.

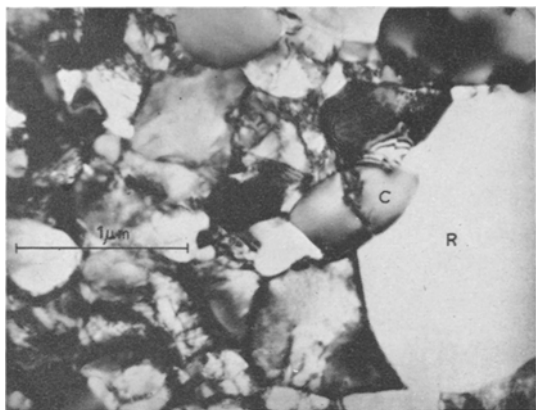


Figure 1 Electron micrograph of a recrystallised grain associated with carbide particles ( $\times 20,000$ ).



Figure 2 Electron micrograph of a recrystallised grain associated with a carbide particle ( $\times 25,000$ ).

grains: this is schematically illustrated in fig. 3. Thus, the latter effect reduces the degree of association between particles and grains, whereas the former increases it. Side effects may also complicate the issue. For instance, an increase in the density of particles may result in a finer grained material [1] due to particle-pinning of grain boundaries, and this in itself will lead to an acceleration of recrystallisation. Consequently, it is difficult to assess the influence of second-phase particles on recrystallisation from a qualitative microscopic examination.

The approach to the problem in this paper is two-fold: firstly the expected associations between carbide particles and recrystallised grains are calculated on the basis of the random appearance of recrystallised grains, and secondly the observed associations are corrected for the sectioning effect. Comparison of these two sets of

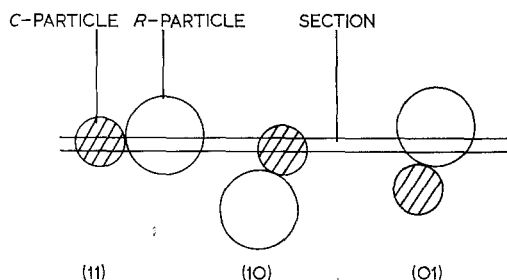


Figure 3 Section associations from a (11) group.

figures allows an assessment of the relationship between carbide particles and recrystallised grains to be made.

## 2. Experimental Techniques

The analysis of the iron-0.4% carbon alloy is given in table I. To produce a uniform dispersion of spheroidal cementite particles the alloy was quenched, tempered, cold-rolled and annealed prior to a final cold rolling reduction of 65%. This processing treatment resulted in an equiaxed ferritic grain structure with a carbide particle mean diameter of  $0.68 \mu\text{m}$  and surface-to-surface spacing in three dimensions of  $2.3 \mu\text{m}$ .

The alloy was annealed at  $480^\circ\text{C}$  for 0.5 min in a salt bath, to produce a volume fraction of recrystallised grains of 0.07. The alloy was then chemically and electrolytically polished to thin sections suitable for transmission electron microscopy.

In the analysis of the results it is necessary to know whether the carbide particles are distributed in the material at random or whether they tend to exist in clumps. The nature of the spatial distribution was determined by taking optical micrographs of several random planes through the material. A grid was marked upon the micrographs, the proportion of squares containing 0, 1, 2 . . . particles was counted and compared with that expected on the basis of a Poisson distribution. The results shown in table II indicate that the carbide particles are randomly distributed in the alloy.

To establish whether the carbide particles are sectioned during electropolishing in the thin section preparation or stand out in relief upon the surface of the section, specimens were allowed to become contaminated in the electron microscope by the deposition of a carbon film. Under these conditions, it has been shown by Sellars and Smith [3] that a halo appears around particles standing out in relief from the surface.

TABLE I Analysis in wt% of iron-carbon alloy

C	Si	Cr	Mo	V	S	Al	Mn	P
0.4	< 0.1	< 0.01	< 0.01	< 0.01	< 0.005	0.008	< 0.1	Not detected

TABLE II

Number of particles in a square, $k$	0	1	2	3	4	5	6
Calculated % of squares containing $k$ particles assuming a random distribution	47	36	13	3	0.6	0.1	0
Observed % of squares containing $k$ particles	51	31	14	4	1	0.1	0.02

Total number of squares = 3,689

Total number of particles = 2,819

This effect was not observed in the current case, nor was any evidence of surface relief due to the particles evident on examination of the material in a Scanning Electron Microscope. It is therefore concluded that particles are sectioned during electro-polishing such that both surfaces of the foil are smooth.

The success of the method clearly depends on the two dissimilar phases being distinguishable from the surrounding medium and each other. Carbide particles were usually distinguishable visually in the electron microscope; on occasions where there was uncertainty, electron diffraction and dark field conditions [4] were employed for positive identification. Recrystallised grains were distinguished from the substructure in the surrounding deformed matrix by their size and low dislocation density.

### 3. Theory

For the purpose of this analysis carbide particles and recrystallised grains will be denoted  $C$ -particles and  $R$ -particles respectively.

Consider a population of  $C$ -particles embedded in a material. A different population of  $R$ -particles is then interspersed at random in the same matrix. The object of the first section of the analysis is to determine the degree of association between the two types of particles.

The analysis may be applied only to systems containing relatively small volume fractions of particles as the expressions are strictly valid only at the limit when the volume fraction of particles goes to zero, keeping their size finite.

#### 3.1. Association due to Random Positioning

The particles are taken to be spherical and are defined by their centres.  $C$ - and  $R$ -particles have radii of  $x$  and  $r$  respectively. The material is di-

vided into cells of volume  $v$ , where

$$v = \frac{4}{3} \pi (r + x)^3 \quad (1)$$

The cell volume, as shown in fig. 4 is chosen such that if an  $R$ -particle centre appears in a cell

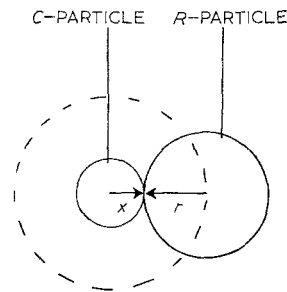


Figure 4 Volume of a cell,  $v$ .

containing a  $C$ -particle at the centre, the two particles will be in contact in three dimensions and this is defined as an association between the particles. The determination of the probabilities of various associations thus reduces to the calculation that certain combinations of particles will be in a cell. This method holds providing both the  $C$ - and  $R$ -particle spacings are larger than the cell diameter, otherwise associations in one cell may overlap and interfere with those in neighbouring cells.

If the  $C$ -particles are randomly distributed in the material then  $p(l)$ , the probability of finding  $l$  particles in a cell of volume  $v$ , is given by the Poisson formula:

$$p(l) = \frac{m^l}{l!} \exp(-m) \quad (2)$$

where the number of particles =  $l = 0, 1, 2, \dots$  and  $m$  is the expected or average number of

particles per cell. The latter quantity is easily calculated from the number of *C*-particles per unit volume,  $N_c$ , and cells per unit volume,  $N$ ,

$$N_c = 3a_c/4\pi x^3$$

where  $a_c$  is the volume fraction of the material occupied by phase *C*.

$$N = 3/4\pi(r + x)^3$$

The expected number of particles in a cell  $m_c$ , is given by

$$m_c = N_c/N = a_c(r + x)^3/x^3 \tag{3}$$

From equation 2 the probability that particles of phase *C* will be in a cell is given by  $p(l)$ ,

$$p(l) = \frac{m_c^l}{l!} \exp(-m_c) \tag{4}$$

where  $l = 0, 1, 2, \dots$ . The *R*-particles are now randomly distributed throughout the material, and the expected number of *R*-particles in a cell is given by  $m_R$ ,

$$m_R = N_R/N = a_R(r + x)^3/r^3 \tag{5}$$

where  $N_R$  is the number of *R*-particles per unit volume and  $a_R$  is the volume fraction of material occupied by phase *R*.

From equation 2, the probability that  $k$  *R*-particles will be in a cell is given by  $p(k)$ ,

$$p(k) = \frac{m_R^k}{k!} \exp(-m_R) \tag{6}$$

where the number of *R*-particles =  $k = 0, 1, 2, \dots$ . Finally, the probability that  $l$  *C*-particles and  $k$  *R*-particles will be in a cell is  $p(lk)$ , where \*

$$\begin{aligned} p(lk) &= p(l) \cdot p(k) \\ &= \frac{m_c^l}{l!} \frac{m_R^k}{k!} \exp(-m_c - m_R) \end{aligned} \tag{7}$$

This is by definition the probability of an association between  $l$  particles of phase *C* and  $k$  particles of phase *R* and will be denoted as an ( $lk$ ) association: the first figure in the bracket referring to the number of *C*-particles and the second figure to the number of *R*-particles in a particular association.

All possible associations between the two types of particles are given by a matrix ( $p_{lk}$ ) where  $l$ ,

$k = 0, 1, 2, 3, \dots$   
i.e.

$$\begin{pmatrix} P_{00} & P_{01} & P_{02} & \dots & P_{0k} \\ P_{10} & P_{11} & P_{12} & \dots & P_{1k} \\ P_{20} & P_{21} & P_{22} & \dots & P_{2k} \\ \dots & \dots & \dots & \dots & \dots \\ \dots & \dots & \dots & \dots & \dots \\ P_{l0} & P_{l1} & P_{l2} & \dots & P_{lk} \end{pmatrix}$$

and the sum of the elements of this matrix will equal unity. Equation 7 gives the probabilities that each of these associations will be formed in a random mixture of particles.

### 3.2. Effects of Sectioning upon Associations

Three-dimensional structures are often studied by observations on planar sections using optical microscopy or thin sections with electron microscopy. For the purposes of this analysis the former is simply a special case of the latter, since it may be considered as a section of zero thickness. Very thin sections of metal are transparent to electrons and so the model to be used is a mixed distribution of spherical particles of two distinct phases embedded in a transparent material from which a slice is cut. The thickness of the slice is taken to be such that overlapping can be ignored, that is, less than twice the average particle diameter.

Associations between particles observed in two-dimensions will be a distorted version of the true three-dimensional associations. By way of illustration, fig. 3 schematically illustrates the effect of sectioning on a (11) association in the bulk material: (11), (10) and (01) associations may be observed in a section. Unless the section passes through the centres of both particles, they will not appear in contact in two dimensions, but their profiles will be in the immediate vicinity of one another and this will still be considered as an association between particles in two dimensions. The associations that may be found in a section clearly depend upon the original association in the bulk material. Sectioning of an ( $lk$ ) association in the bulk material will result in associations given by the elements of the matrix ( $P_{ij}$ ) where  $i = 0, 1, 2, \dots, l$  and  $j = 0, 1, 2, \dots, k$ . The

\*Equations 4, 6 and 7 hold only for low values of  $l$  and  $k$ , since the presence of many particles in a cell will significantly reduce the free volume in the cell and hence the probability of obtaining a further particle in it. (In the current experiment, the *R*-particles tend to nucleate simultaneously in small volumes throughout the material and then grow to a radius  $r$ . Consequently, during the nucleation or positioning stage, the reduction in cell free volume due to other *R*-particles is small).

probabilities of obtaining each of these section associations are again dependent upon the association type originally present in three-dimensions. The sectioning of each of the various types of association will now be considered.

### 3.2.1. Sectioning of (1k) Groups

One particle of phase C with  $k$  particles of phase R associated with it in the bulk material is defined as a (1k) group or association. A two-dimensional representation of a (1k) arrangement is shown in fig. 5: C-particle centred at the origin,

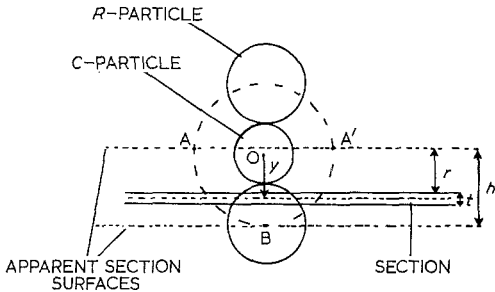


Figure 5 A (1k) configuration sectioned in the range  $|x + t/2| < y < |2r + x + t/2|$ .

surrounded by R-particles. The centres of the R-particles may be anywhere on the dotted circle, all positions being equally likely. All particles in the group are in contact with a dissimilar particle.

If the above group is sectioned at random, one of a number of different associations between the two types of particles will be obtained in the section. All possible associations are given by the elements of the matrix  $(f_{ij})$  where  $i = 0, 1$  and  $j = 0, 1, 2 \dots k$ , that is

$$\begin{pmatrix} f_{00} & f_{01} & f_{02} & \dots & f_{0k} \\ f_{10} & f_{11} & f_{12} & \dots & f_{1k} \end{pmatrix}$$

If  $y$  is the distance of the middle of the section from the origin, the first row of this matrix will be obtained for  $|x + t/2| < y < |2r + x + t/2|$  and the second row for  $0 < y < |x + t/2|$ . In the latter range, fig. 5 shows that the section will always contain a C-particle, but may or may not contain R-particles: associations of the type (1j), where  $j = 0, 1, 2 \dots k$  will be obtained. In the former range, the C-particle will never be sectioned, although R-particles may appear in the section: associations of the type (0j), where  $j = 0, 1, 2 \dots k$  will be established. The probabilities of obtaining each of the possible associations for the above  $y$  ranges in a section

thickness  $t$ , will now be derived.

*Section in the range  $0 < y < |x + t/2|$*

Calculations of the probability  $u$  that an R-particle will be sectioned and thus be associated with the C-particle in the section, is divided into two parts depending on whether both surfaces or only one surface of the section intersect the particle.

Part I applies to the range  $0 < y < |x - t/2|$

Part II applies to the range

$$|x - t/2| < y < |x + t/2|$$

*Part I:*

Fig. 6 is a representation of the section in this range and it is evident that if an R-particle centre

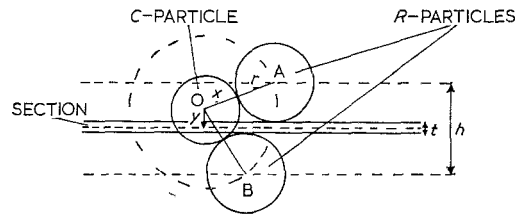


Figure 6 Limiting positions for an R-particle to be in the section ( $0 < y < x - t/2$ ).

lies between A and B then part of the particle will appear in the section adjacent to the C-particle. The dotted lines through A and B indicate the "apparent section surfaces" and the spacing  $h$  between them as the "apparent section thickness", since if a grain centre lies between the apparent section surfaces it will be represented in the section.

The R-particle centres may lie anywhere on the surface of the dotted sphere, centre O, radius  $(r + x)$ ; an R-particle will be sectioned if its centre is on the surface of this sphere between the apparent section surfaces, i.e. the surface generated by rotating AB about the  $y$ -axis. The probability  $u$ , of this event is the latter area over the total surface area of the sphere radius  $(r + x)$ .

Now the surface area  $A$  of a section of a sphere of radius  $R$  cut by two parallel faces is given by,

$$A = 2\pi Rh \quad (8)$$

where  $h$  is the distance apart of the faces, which in this instance is the apparent section thickness.

From fig. 6:

$$h = (2r + t)$$

$$R = (r + x)$$

Therefore

$$A = 2\pi(r + x)(2r + t)$$

The probability that a particular *R*-particle will be associated with the *C*-particle in the section is given by  $u_1$ ,

$$u_1 = \frac{A}{4\pi(r + x)^2} = \frac{2r + t}{2(r + x)} \quad (9)$$

*Part II:*

Fig. 7 illustrates the section in this range and CDE describes the range over which part of an *R*-particle will appear in the section associated with the *C*-particle. The centre of an *R*-particle must therefore lie on the surface of the spherical cap CDE cut by the apparent section surfaces. The probability  $u_2$  of occurrence of this event is the latter area *A*, over the total surface area of the sphere radius  $(r + x)$ .

From fig. 7:

$$h = 2r + x + t/2 - y$$

$$R = (r + x)$$

From equation 8

$$A = 2\pi(r + x)(2r + x + t/2 - y)$$

hence

$$u_2 = \frac{A}{4\pi(r + x)^2} = \frac{2r + x + t/2 - y}{2(r + x)} \quad (10)$$

$u_2$  is thus a linear function of  $y$ .

To determine an average probability over parts I and II in the range  $0 < y < |x + t/2|$  the mean value  $u$  is taken,

$$u = \frac{1}{x + t/2} \left( \int_0^{x-t/2} u_1 dy + \int_{x-t/2}^{x+t/2} u_2 dy \right)$$

From equations 9 and 10,

$$u = \frac{2rx + t(r + x)}{2(r + x)(x + t/2)} \quad (11)$$

(as expected, the above equation indicates that  $u$  reduces to  $u_1$  at  $t = 0$ ).

Equation 11 gives the mean probability that a particular *R*-particle is associated with the *C*-particle in the section. However, there are  $k$  *R*-particles associated with the *C*-particle in three dimensions and the probability that any  $j$  of these will be in the section is given by the binomial distribution as\*:

$$\binom{k}{j} u^j (1 - u)^{k-j} \quad (12)$$

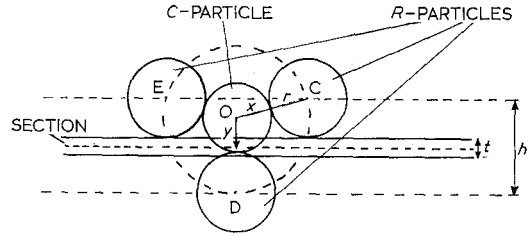


Figure 7 Limiting positions for an *R*-particle to be in the section  $(x - t/2 < y < x + t/2)$ .

where  $j = 0, 1, 2, \dots, k$ . This expression gives the probability that  $j$  *R*-particles will be associated with the *C*-particle in the section.

The complete sectioning range over which part of the  $(1k)$  group in the bulk material range may be sectioned is

$$-(2r + x + t/2) < y < (2r + x + t/2),$$

and the probability that a section will be in the range  $0 < y < |x + t/2|$  is  $(2x + t)/(4r + 2x + t)$ . The overall probability  $P(1j)$  of a  $(1j)$  association in the section, resulting from sectioning a  $(1k)$  group in the bulk material, is given by the product of the latter probability and equation 12, i.e.

$$P(1j) = \left( \frac{2x + t}{4r + 2x + t} \right) \binom{k}{j} u^j (1 - u)^{k-j} \quad (13)$$

where  $j = 0, 1, 2, \dots, k$ .

If a bulk material containing  $(1k)$  associations is sectioned, the proportion of  $(1j)$  associations in the section will be given by  $P(1j)$ .

*Section in the range*

$$|x + t/2| < y < |2r + x + t/2|$$

Fig. 5 illustrates the section lying in the above range and it is clear that while *R*-particles may be sectioned the *C*-particle will not. As a result associations of the type  $(0j)$ ,  $j = 0, 1, 2, \dots, k$  will be found in a section.

The probability  $w$  that an *R*-particle will be sectioned is calculated in a similar manner as  $u$ . An *R*-particle will be sectioned providing its centre lies between the apparent section surfaces. In three-dimensions the centre must lie on the cap  $AB\hat{A}$  (fig. 5). The probability  $w$ , of the latter occurrence is the area of the cap  $AB\hat{A}$  over the surface of the sphere, radius  $(r + x)$ .

The apparent section thickness

$$h = 2r + x + t/2 - y.$$

\*This holds only for low values of  $k$ , since the presence of one *R*-particle in the section reduces the effective value of  $A$  in equation 8. As a result the probability of obtaining a second *R*-particle associated with the *C*-particle in the section is less than  $u$ . Conversely, the absence of an *R*-particle in the section increases this probability.

From equation 8, area of  $AB\bar{A}$  is

$$A = 2\pi(r+x)(2r+x+t/2-y)$$

hence  $w_1$

$$= \frac{2r+x+t/2-y}{2(r+x)}$$

$w_1$  is a function of  $y$ , the mean value is given by  $w$ ,

$$w = \frac{1}{2r} \int_{x+t/2}^{2r+x+t/2} \left( \frac{2r+x+t/2-y}{2(r+x)} \right) dy$$

hence

$$w = \frac{r}{2(r+x)} \quad (14)$$

Thus, the probability that  $k$   $R$ -particles will be in the section is given by,

$$\binom{k}{j} w^j (1-w)^{k-j}$$

where  $j = 0, 1, 2, \dots, k$ ; the probability that a section is in the range

$$|x+t/2| < y < |2r+x+t/2|$$

is  $4r/4r+2x+t$ .

The overall probability that a section from a  $(1k)$  group in the bulk material will contain a  $(0j)$  association is given by  $P(0j)$ ,

$$P(0j) = \frac{4r}{4r+2x+t} \binom{k}{j} w^j (1-w)^{k-j} \quad (15)$$

Equations 13 and 15 give the probabilities of obtaining all the possible section associations resulting from the sectioning of a  $(1k)$  configuration in the bulk material.

### 3.2.2. Sectioning of $(l1)$ Groups

An  $(l1)$  group in the bulk material is a configuration with one  $R$ -particle together with  $l$  associated  $C$ -particles. This is the transpose of the  $(1k)$  type of association, the  $C$ - and  $R$ -particles simply being interchanged. Consequently, the equations are the same as for the  $(1k)$  group, with  $r$  and  $x$  interchanged.

Thus, from equation 11 the probability that a particular  $C$ -particle will be associated with the  $R$ -particle in the section is given by  $\dot{u}$ ,

$$\dot{u} = \frac{2rx+t(r+x)}{2(r+x)(r+t/2)} \quad (16)$$

and from equation 13 the probability that a section from an  $(l1)$  group in the bulk material contains an  $(i1)$  association is

$$P(i1) = \frac{2r+t}{4x+2r+t} \binom{l}{i} \dot{u}^i (1-\dot{u})^{l-i} \quad (17)$$

where  $i = 0, 1, 2, \dots, l$ . Following equation 14 the probability of an  $(i0)$  association in the section is given by  $\dot{w}$ ,

$$\dot{w} = \frac{x}{2(r+x)} \quad (18)$$

and from equation 15 the probability that a section from an  $(l1)$  group contains an  $(i0)$  association is given by  $P(i0)$ ,

$$P(i0) = \frac{4x}{4x+2r+t} \binom{l}{i} \dot{w}^i (1-\dot{w})^{l-i} \quad (19)$$

where  $i = 0, 1, 2, \dots, l$ . Equations 17 and 19 give the probabilities of obtaining all the possible section associations arising out of sectioning an  $(l1)$  configuration in the bulk material.

In summary, sectioning probabilities for groups of the type  $(1k)$  and  $(l1)$ , that is the first two rows and columns of the general  $P(lk)$  matrix, have been derived.

### 3.2.3. Sectioning of $(lk)$ Groups

The principles involved in the derivation of the sectioning probabilities for  $(lk)$  groups ( $l, k > 1$ ) are the same as for  $(1k)$  groups, but owing to the greater complexity of the configurations the calculations are more complicated. In the current experimental investigation the most complex association observed was  $(22)$ . The sectioning probabilities for the latter association have been calculated elsewhere [5] and in order to limit the length of the current discussion the final expressions will simply be quoted here. These expressions strictly apply to the planar section case ( $t = 0$ ), but may be used for systems where the section thickness is small compared with the average particle diameter.

$$P(22) = \frac{r\dot{u}^2}{4(r+x)} \quad (20)$$

where  $\dot{u}$  is given by equation 16 when  $t = 0$ , as

$$\dot{u} = \frac{x}{r+x} \quad (21)$$

$$P(12) = \frac{2r\dot{u}(1-\dot{u})}{4(r+x)} \quad (22)$$

$$P(02) = \frac{r(1-\dot{u})^2}{4(r+x)} \quad (23)$$

$$P(21) = \frac{2r\dot{q}\dot{u}}{4(r+x)} \quad (24)$$

where

$$q = \frac{x^2}{4r(r+x)} \left( 3 + 2 \log_e \left( \frac{r}{x} \right) \right) \quad (25)$$

$$P(11) = \frac{2r\dot{u}(1-q) + 2rq(1-\dot{u})}{4(r+x)} \quad (26)$$

$$P(01) = \frac{2r(1-\dot{u})(1-q)}{4(r+x)} \quad (27)$$

$$P(20) = \left( \frac{x}{r+x} \right) g^2 + \frac{rq^2}{4(r+x)} \quad (28)$$

where

$$g = \frac{x^2}{8r(r+x)}$$

$$P(10) = \left( \frac{x}{r+x} \right) 2g(1-g) + \frac{2rq(1-q)}{4(r+x)} \quad (29)$$

$$P(00) = \left( \frac{x}{r+x} \right) (1-g)^2 + \frac{r(1-q)^2}{4(r+x)} \quad (30)$$

To conclude, expressions have been derived in section 3.1 to determine the expected associations due to random mixing and in section 3.2 to relate the apparent associations to real three-dimensional configurations. The equations refer to the general case of a section of thickness  $t$ , but may be applied to the particular case of a planar section by equating  $t$  to zero.

In an experimental investigation to determine the association between particles, the data required is the section thickness, volume fraction and radii of each phase. Randomly selected areas of the material are examined and the frequencies of the various associations recorded. The observed associations are then transformed to three-dimensional associations and compared with the random case. If the experimental frequencies are significantly higher than random, there will be a positive association between particles (in the current system this would imply that carbide particles stimulated the nucleation of recrystallised grains) whereas if they are below random there will be a negative association between particles (that is, particles inhibit recrystallisation).

#### 4. Results

The radii of carbide particles and recrystallised grains observed in thin sections in the electron microscope were 0.28 and 0.50  $\mu\text{m}$  respectively. After correction for sectioning [6] these figures

become 0.34 and 0.62. The volume fractions of carbide particles and recrystallised grains were 0.05 and 0.07 respectively. The foil thickness was determined [4] to be 0.10  $\mu\text{m}$ .

Since it has been shown that the carbide particles are randomly distributed in the material, equation 7 may be applied to determine the expected associations between particles due to random positioning. Substitution of the above data in this equation gives the relative frequencies of random associations as:

	(01)	(02)	(03)	
	0.088	0.011	0.001	
(10)	(11)	(12)	(13)	
0.386	0.096	0.012	0.001	
(20)	(21)	(22)	(23)	(31)
0.212	0.053	0.007	0.001	
(30)	(31)	(32)		
0.078	0.019	0.003		
(40)	(41)	(42)		
0.024	0.005	0.001		
(50)	(51)			
0.003	0.001			

where  $(lk)$  denotes an association between  $l$  C-particles and  $k$  R-particles. Associations with frequencies of less than 0.0005 are not included in the above matrix.

Experimentally, the following relative frequencies for the various associations were observed on examining thin sections of the partially recrystallised alloy in the electron microscope. This data was obtained from a total of 485 independent associations.

	(01)	(02)	(03)	(04)	(05)
	0.124	0.039	0.029	0.01	—
(10)	(11)	(12)	(13)	(14)	(15)
0.375	0.233	0.080	0.008	0.004	0.002
(20)	(21)	(22)			
0.017	0.052	0.016			
(30)	(31)				
0.004	0.002				
(40)					
—					
(50)					
0.002					

To transform the above results into three-dimensional associations, the most complex association observed is assumed to be the most complex association in the bulk material. The contributions to lower order associations from this association are then calculated and subtracted from the observed frequencies. This process is repeated, making the same assumptions about the next most complex association



and so on until a corrected matrix of associations is obtained. A numerical example of this procedure is given in [5]. The fully corrected results are:

$$\begin{array}{ccccc}
 (01) & (02) & (03) & (04) & (05) \\
 \text{---} & \text{---} & 0.018 & 0.007 & \text{---} \\
 (10) & (11) & (12) & (13) & (14) & (15) \\
 0.206 & 0.066 & 0.075 & 0.031 & \text{---} & 0.039 \\
 (20) & (21) & (22) & & & \\
 0.002 & 0.161 & 0.361 & & & \\
 (30) & (31) & & & & \\
 0.003 & 0.034 & & & & \\
 (40) & & & & & \\
 \text{---} & & & & & \\
 (50) & & & & & \\
 0.002 & & & & & 
 \end{array} \quad (33)$$

## 5. Discussion

In the alloy investigated the average centre-to-centre spacing in three dimensions of  $3 \mu\text{m}$  between carbide particles does not greatly exceed the cell diameter ( $1.9 \mu\text{m}$ ), and therefore events in one cell may interfere with those in neighbouring cells. The results must therefore be considered with this in mind. It is possible, depending on the relative spatial orientations, that a (11) association will impinge upon another (11) association to give an apparent (22) association, since the surface-to-surface carbide particle spacing ( $2.3 \mu\text{m}$ ) is the same order of magnitude as twice the recrystallised grain diameter ( $2.6 \mu\text{m}$ ). On the other hand, it is unlikely that a (11) association will impinge upon carbide particles to give an (11) association so that the latter associations may be considered to give valid information concerning the nucleation stage. The spacing between recrystallised grains is double that of the carbide particle spacing and consequently the (1*k*) associations are again meaningful in the context of nucleation.

Matrix 31 gives the frequencies of expected associations due to random positioning, whereas matrix 33 shows the actual associations between particles and grains in the material. Real associations between particles and grains exist when both *l* and *k* are finite in a (*lk*) association: that is the interior elements of the matrix. For the observed results the sum of these elements in matrix 33 is:

$$\sum P(lk) = 0.767$$

for *l, k* > 0 and for the random associations given by matrix 31,

$$\sum P(lk) = 0.199$$

for *l, k* > 0.

It is therefore clear that the associations observed in the iron-0.4% carbon alloy between carbide particles and recrystallised grains are much higher than random, indicating that carbide particles are nucleation sites for recrystallised grains. The reasons for this behaviour have been discussed [2] in terms of the stress concentrations that build up around particles due to the markedly different deformation characteristics of the carbide and  $\alpha$ -iron phases. The result is a more complex deformation pattern in the  $\alpha$ -iron around the particles leading to greater misorientations in the sub-structure which facilitate the development of recrystallisation nuclei.

The frequencies of (0*k*) associations observed are much less than random (0.025 compared with 0.100); this indicates that virtually all recrystallised grains are adjacent to carbide particles. Carbide particles are therefore the exclusive nucleation sites for recrystallised grains up to 7% recrystallisation.

However, the transpose of the above situation is not true, in that all carbide particles are not associated with recrystallised grains. From matrix 33, the observed frequency of (0) associations is 0.213 and so 0.17 of particles do not nucleate grains. This suggests there is a criterion that particles must satisfy to act as nucleation sites. Closer examination of the results revealed that the average diameter of carbide particles associated with recrystallised grains was  $0.74 \mu\text{m}$  (105 particles measured) while that for particles apparently dissociated from grains was  $0.66 \mu\text{m}$  (126 particles measured). It may be shown from matrices 32 and 33 that 70% of the latter particles were originally adjacent to grains in three-dimensions. Assuming this percentage of particles have a mean diameter of  $0.74 \mu\text{m}$  then the real diameter of dissociated particles will be approximately  $0.45 \mu\text{m}$ . These results suggest the existence of a critical particle size for the nucleation of recrystallisation.

It is now generally accepted that the nuclei for recrystallisation are subgrains produced in the deformation process. Goodier [7] has calculated that stress concentrations are only appreciable up to one particle diameter from the particle surface and so it seems likely that a particle can only act as a nucleation site if this affected volume is large enough to contain a subgrain. The minimum particle size for particle-aided nucleation of

recrystallisation would, on this basis, be of the same order of magnitude as the subgrain size. The average subgrain diameter in the iron-0.4% carbon alloy cold-rolled 65% is 0.5  $\mu\text{m}$  and it is proposed that the 17% of particles which do not act as recrystallisation sites, are below this size.

The observed frequencies of (12), (13) and (15) associations shown in matrix 33 are markedly higher than random (0.145 as opposed to 0.013): 9.2% of carbide particles nucleate two or more recrystallised grains. It is therefore clear that certain particles are more powerful nucleation sites than others. To gain further information sixteen ( $1k$ ) associations where  $k > 1$  were examined in detail in the electron microscope and it was found that eleven were in contact with grain boundaries. The high nucleation efficiency of these carbide particles is attributed to the presence of grain boundaries for the complexity of the deformation around the latter augments that associated with the particles to give a higher level of deformation in the immediate vicinity, and thus a high nucleation rate of recrystallised grains.

As discussed previously, impingement of neighbouring (11) associations to form (22) associations is likely to occur in this material, with the result that the (11) frequency will be artificially low and the (22) frequency artificially high. However, the (20) association frequency is much less than random (0.002 as opposed to 0.212) and in principle the balance should be found in the (21) and (22) frequencies. It is therefore likely that the high (22) frequency is in part a nucleation effect. The (21) and (31) association frequencies observed in the material are substantially higher than random, while the (30), (40), (50) frequencies are correspondingly lower than random (0.007 compared with 0.317). However, it is notable that the observed (10) association frequency does not fall to a similarly low value (0.206 compared to a random level of 0.386). This collection of results indicates that the presence of a group of carbide particles in close proximity leads to an enhancement in the recrystallised grain formation. In the material examined, this may be explained on the basis that the stress fields of carbide particles in close proximity combine to give a higher level of deformation in the immediate vicinity and hence a higher recrystallisation tendency than that adjacent to a single particle.

Since the carbide particle distribution is the same in both the random and experimental systems, the row totals of matrices 31 and 33 should be equal. However, owing to the impingement of associations this is not the case.

## 6. Conclusions

(a) An analysis has been derived to determine the associations between particles of two phases due to random positioning and to transform associations observed in thin or planar sections to three-dimensional associations. The expressions enable the real degree of association between particles to be assessed.

(b) The analysis has been applied to an iron-0.4% carbon alloy and demonstrates that carbide particles are nucleation sites for recrystallisation.

(c) Carbide particles in the above alloy are shown to be the exclusive nucleation sites for recrystallised grains during the early stages of recrystallisation.

(d) The results suggest there is a critical particle size necessary for nucleation of recrystallisation and it is proposed that this is equal to the subgrain diameter.

(e) Particles on grain boundaries are stronger nucleation sites than those in grain interiors.

(f) Particles in close proximity enhance the recrystallisation tendency of the immediate matrix.

## References

1. R. W. CAHN, "Physical Metallurgy" (North-Holland, Amsterdam, 1965) p. 925.
2. D. T. GAWNE and G. T. HIGGINS, "Textures in Research and Practice" (Springer-Verlag, Berlin, 1969) p. 319.
3. C. M. SELLARS and A. F. SMITH, *J. Mater. Sci.* **2** (1967) 521.
4. P. B. HIRSCH, A. HOWIE, R. B. NICHOLSON, D. W. PASHLEY, and M. J. WHELAN, "Electron Microscopy of Thin Crystals" (Butterworths, New York, 1965).
5. D. T. GAWNE, Ph.D. Thesis, University of Liverpool, 1969.
6. P. L. GOLDSMITH, *Brit. J. Appl. Phys.* **18** (1967) 813.
7. J. N. GOODIER, *Trans. ASM* **55** (1933) 39.

Received 14 October 1970 and accepted 10 March 1971.